Supporting Information

Nanocellulose-Short Peptide Self-Assembly for Improved Mechanical Strength and Barrier Performance

Alessandro Marchetti,[a,‡] Elisa Marelli, [a,‡] Greta Bergamaschi,[b] Panu Lahtinen,[c] Arja Panaanen,[c] Markus Linder,[d] Claudia Pigliacelli,[a,] Pierangelo Metrangolo[a,*]*

[a]Laboratory of Supramolecular and Bio-Nanomaterials (SBNLab), Department of Chemistry, Materials, and Chemical Engineering "Giulio Natta", Politecnico di Milano, Via L. Mancinelli 7, 20131 Milano, Italy.

[b]Istituto di Scienze e Tecnologie Chimiche, National Research Council of Italy, Via M. Bianco 9, 20131 Milano, Italy.

[c]VTT Technical Research Centre of Finland Ltd, Tekniikantie 21, 02150 Espoo, Finland.

[d]Department of Bioproducts and Biosystems, School of Chemical Engineering, Aalto University, Kemistintie 1, 02150 Espoo, Finland.

1. Materials

1.1. Peptide synthesis: general procedures

Resin loading

2-CTC (2-chlorotrityl chloride) resin (0.5 mmol/g loading) was swollen in dichloromethane (CH_2Cl_2) for 30 min. A solution of entering Fmoc- amino acid and N,N-diisopropylethylamine (DIEA) (1.2:8 eq over resin loading) in CH_2Cl_2 (3 mL) was added and the resin shaken at rt for 4 h. The resin was washed with dimethylformamide (DMF) (2 × 3 mL) and capping was
performed by treatment with acetic anhydride/DIEA in CH_2Cl_2 (1 x 30 min). The resin was then washed with DMF (2 × 3 mL), CH_2Cl_2 (2 × 3 mL), and DMF (2 × 3 mL). The resin was subsequently submitted to fully automated iterative peptide assembly (Fmoc-SPPS).

Peptide Assembly via Iterative Fully Automated Microwave Assisted SPPS

Peptides were assembled by stepwise microwave-assisted Fmoc-SPPS on a Biotage ALSTRA Initiator+ peptide synthesizer, operating in a 0.1 mmol scale. Activation of entering Fmoc-protected amino acids (0.3M solution in DMF) was performed using 0.5M ethyl cyanohydroxyiminoacetate (Oxyma) in DMF / 0.5M N,N'-diisopropylcarbodiimide (DIC) in DMF (1:1:1 molar ratio), with 5 equivalents excess over the initial resin loading. Coupling steps were performed for 30 minutes at 50°C. Fmoc-deprotection steps were performed by treatment with a 20% piperidine solution in DMF at room temperature (1x 10 min). Following each coupling or deprotection step, peptidyl-resin was washed with DMF (4 x 3.5 mL). Upon complete chain assembly, resin was washed with CH_2Cl_2 (5 x 3.5 mL) and gently dried under a nitrogen flow.

Cleavage from the Resin

Resin-bound peptide was treated with an ice-cold trifluoroacetic acid (TFA), triisopropylsilane (TIS), water, thioanisole mixture (90:5:2.5:2.5 v/v/v/v, 4mL). After gently shaking the resin for 2 hours at room temperature, the resin was filtered and washed with neat TFA (2 x 4 mL). The combined cleavage solutions were worked-up as indicated below.

Work-up and Purification

Cleavage mixture was concentrated under nitrogen stream and then added dropwise to ice cold diethyl ether (40 mL) to precipitate the crude peptide. The crude peptide was collected by centrifugation and washed with further cold diethyl ether to remove scavengers. Residual diethyl ether was removed by a gentle nitrogen stream and the crude peptide was purified by reversed-phase high performance liquid chromatography (RP-HPLC) and pure fractions combined and analysed by electro-spray ionization mass spectrometry (ESI-MS).

RP-HPLC analysis and purification

Analytical RP-HPLC was performed on a Shimadzu Prominence HPLC (Shimadzu) using a Shimadzu Shimpack GWS C18 column (5-micron, 4.6 mm i.d. x 150 mm). Analytes were
eluted using a binary gradient of mobile phase A (100% water, 0.1% trifluoroacetic acid) and mobile phase B (30% water, 70% acetonitrile, 0.1% trifluoroacetic acid) using the following chromatographic method: 10% B to 100% B in 14 min; flow rate, 1 ml/min. Preparative RP-HPLC was performed on a Shimadzu HPLC Prominence system using a Gemini, Shimadzu,C18 column (10 micron, 21.2 mm i.d. x 250 mm) using the following chromatographic method: 0% B to 90% B in 45 min; flow rate, 14 ml/min. Pure RP-HPLC fractions were combined and lyophilized.

Electro-spray ionization mass spectrometry (ESI-MS)

Electro-spray ionization mass spectrometry (ESI-MS) was performed using a Bruker Esquire 3000+ instrument equipped with an electro-spray ionization source and a quadrupole ion trap detector (QITD).

Table S1. Peptide synthesis characterization: HPLC retention times, purity and m/z detected.

Peptide	R_f (min)	HPLC purity (%)	ESI-MS found
DFNKF	8.28	>98	670.5
DF(I)NKF	9.49	>99	796.3
DF(F_5)NKF	9.35	>96	760.5

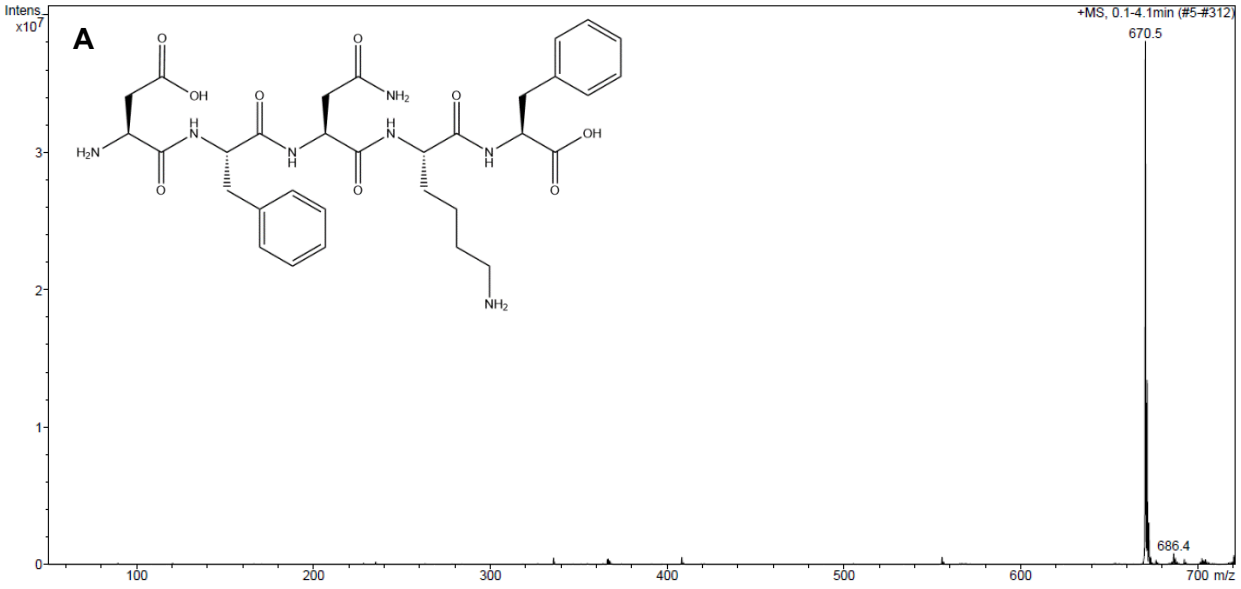

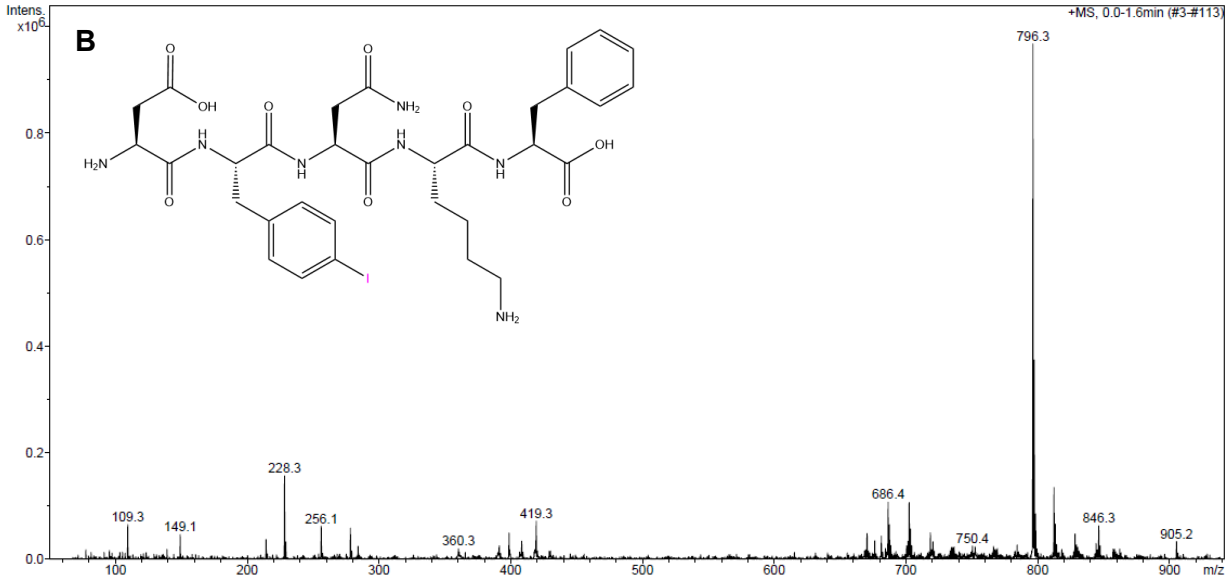

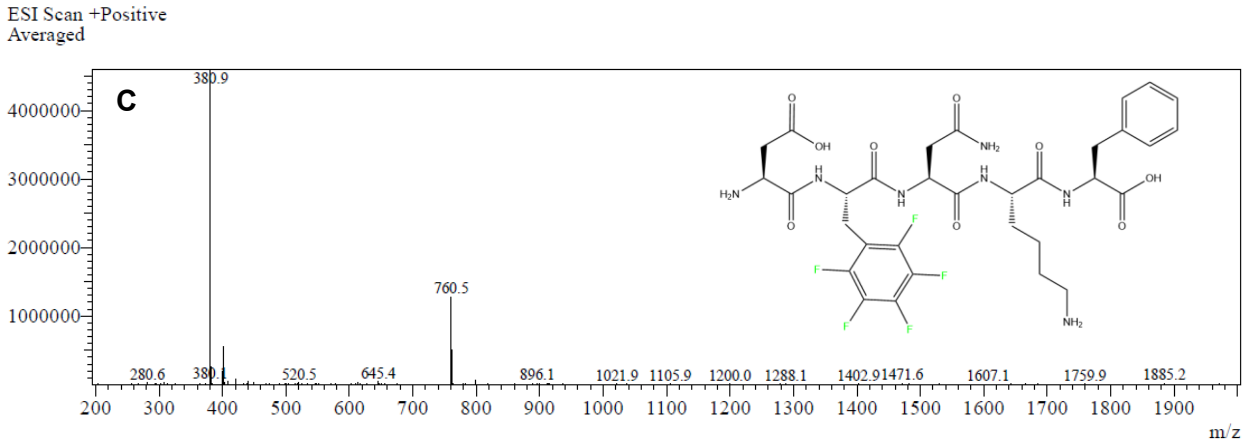

Figure S1. ESI-MS for DFNKF (A), DF(I)NKF (B) and DF(F_5)NKF (C) (positive ion mode).

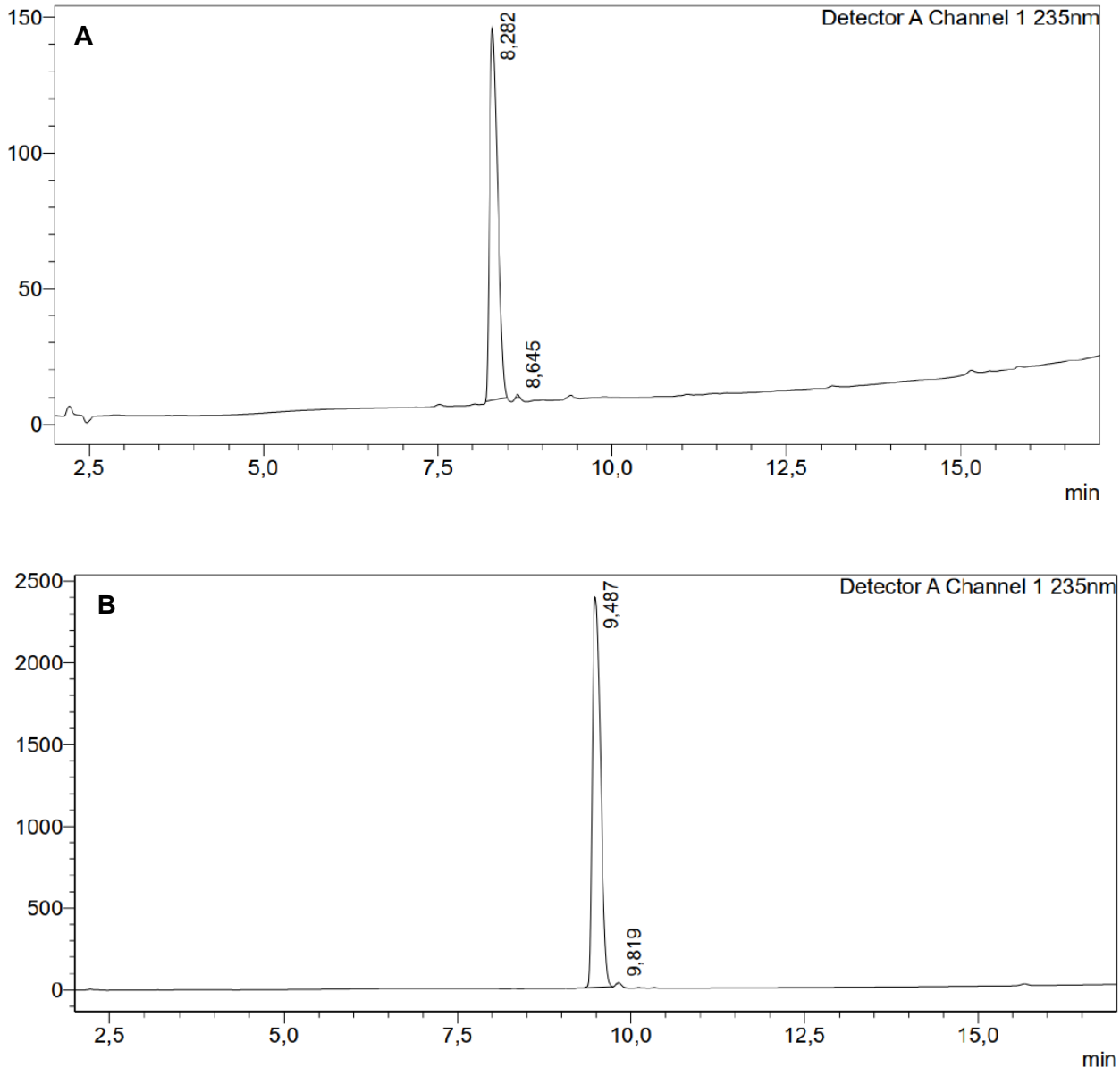

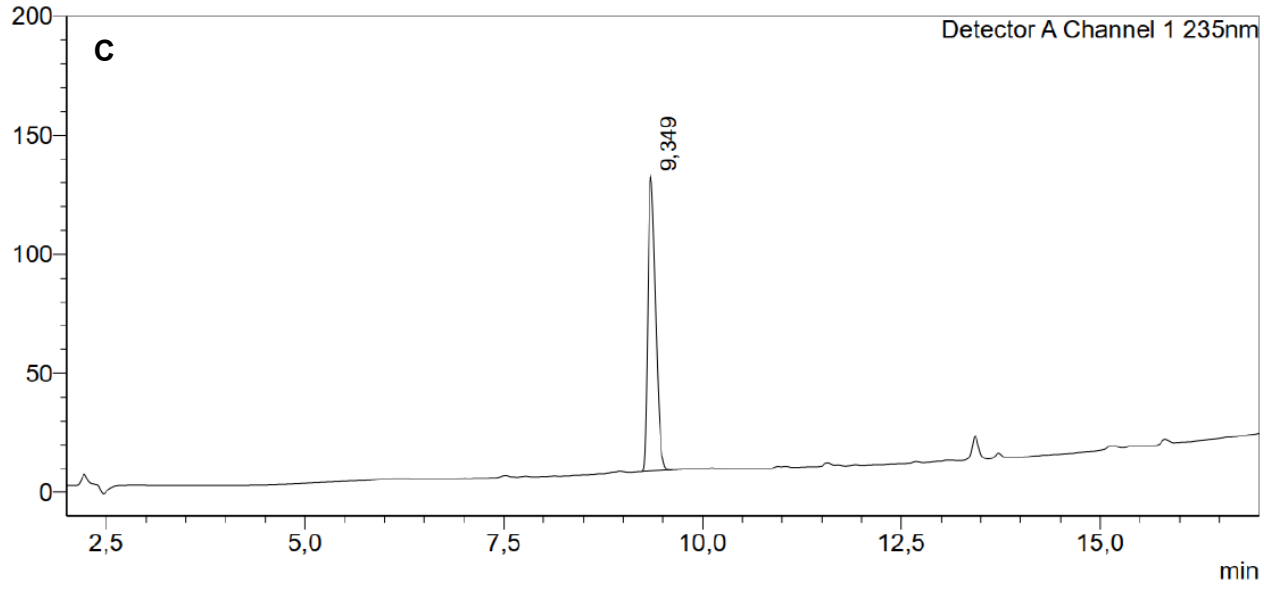

Figure S2. HPLC chromatograms of A) DFNKF, B) DF(I)NKF and C) DF(F_5)NKF.

2. Additional experimental procedures

2.1 . ζ potential measurements

Zeta (ζ) potential measurements were performed with a Malvern Zetasizer Nano ZS diluting ten times the initial samples with MilliQ water. Average potential at the slipping plane was obtained using the Smoluchowski correlation. The temperature was kept at 25 °C and the sample was left equilibrating 60 second before each measurement. Each sample was analysed three times and the results were averaged.

2.2 Transmission Electron Microscopy (TEM)

TEM images were collected using Philips CM200 field emission microscope operated at 200 kV in bright field mode with Omega-type Zero-loss energy filter. The samples were prepared placing on a 200-mesh carbon film-coated grid 10 µL of each hydrogel (previously diluted 1:10) and the exceeding water was removed with filter paper after 1 minute to prevent aggregation effects promoted by drying.

2.3 Attenuated Total Reflectance Fourier-Transform Infrared Spectroscopy (ATR-FTIR)

FT-IR measurements were performed on lyophilized samples in attenuated total reflectance (ATR) mode by using a Nicolet iS50 FT-IR spectrometer equipped with an ATR device. Spectra were collected in the medium IR region (64 scans, 4000–400 cm^{-1}). All the spectra were measured with a resolution of ± 1 cm^{-1} and corrected for the air background.

2.4 Powder X-ray Diffraction (PXRD)

PXRD was performed after lyophilization of the nanocellulose suspensions. Data were collected at room temperature on Bruker AXS D8 powder diffractometer with experimental parameters as follows: Cu-Kα radiation (λ = 1.5418 Å), scanning interval 5-50° at 2θ, step size 0.015°, exposure time 6 s per step.

2.5 Thermogravimetric Analysis (TGA)

The thermal stability of the samples in both their hydrogel and film form was evaluated through thermogravimetric analysis (TGA) using a TGA Q500 V20.13 Build 39, operating in a temperature range between 25°C and 500°C at a 20°C/min heating rate.

Supplementary figures and tables

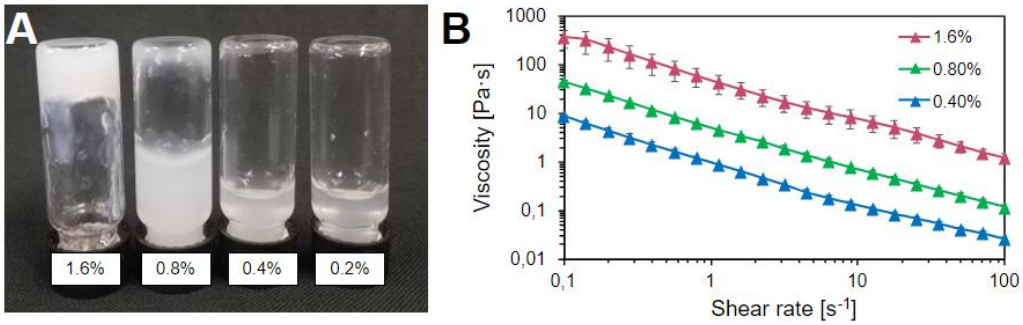

Figure S3. Pictures of CNF suspensions with progressively lower dry matter content (A) and flow curve measurements of CNF dispersions with different solid contents (B).

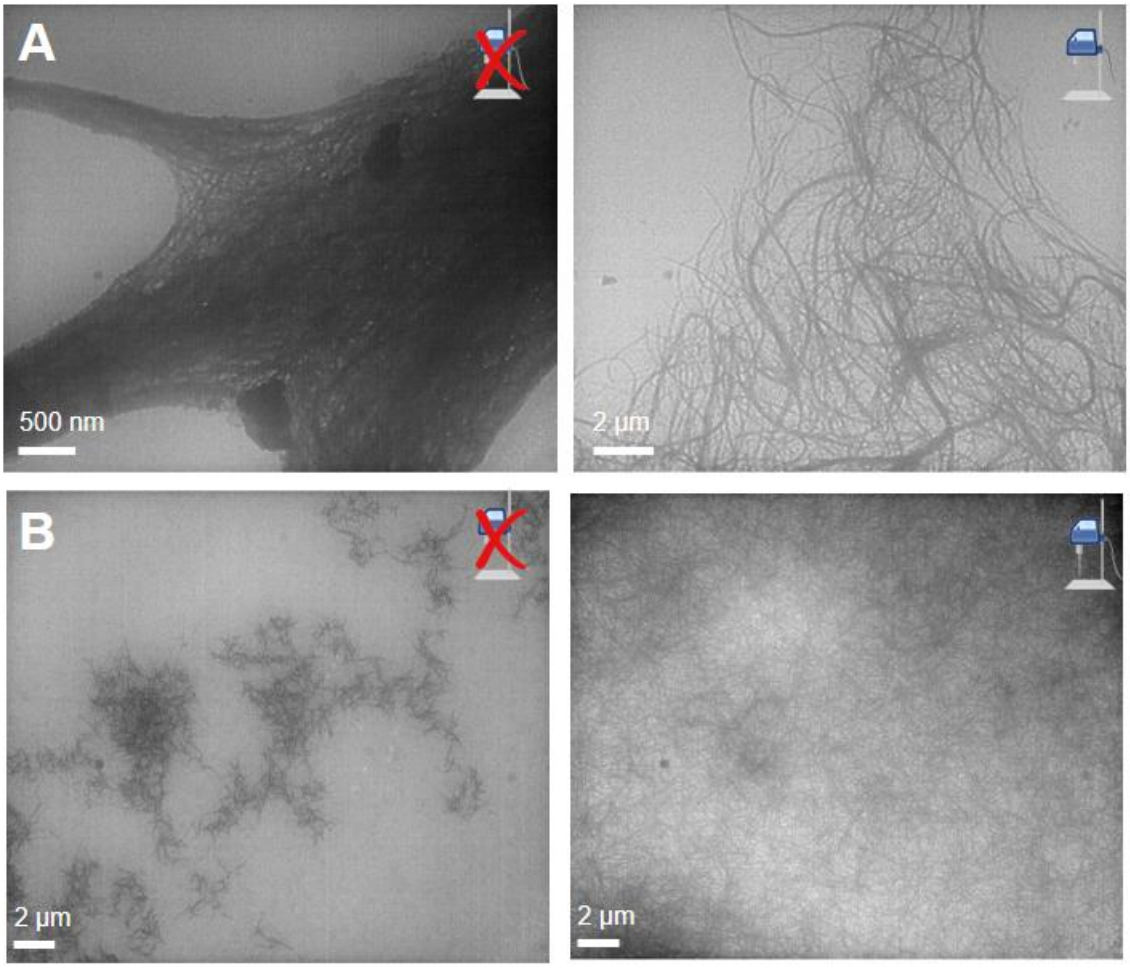

Figure S4. TEM images showing the effect of sonication on neat CNF (A) and on a 0.05% w/w DF(I)NKF solution (B).

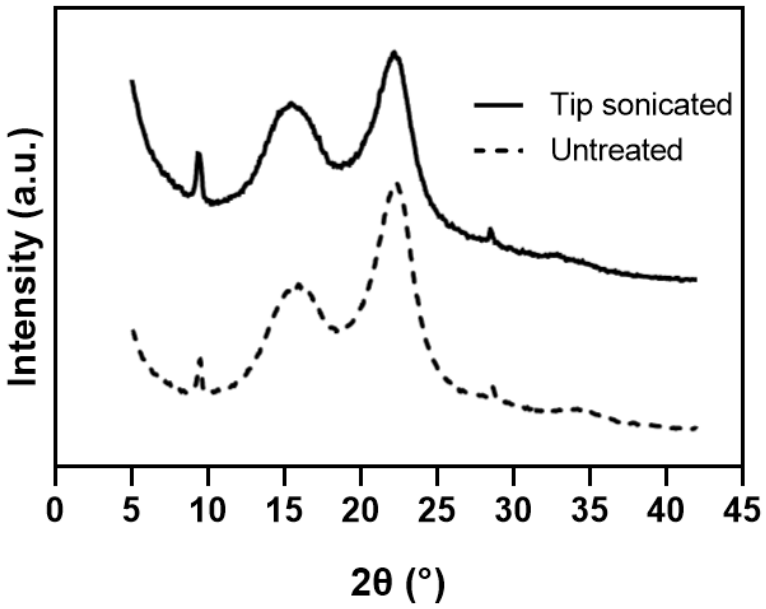

Figure S5. PXRD diffraction pattern of lyophilized CNFs before and after the sonication treatment, showing a diffraction pattern typical of freeze-dried cellulosic materials, with well-defined peaks at 22° and 16° corresponding to the (002) and (001) planes, respectively.[S1] The cristallinity index (CI) of the samples under analysis was determined according to the equation below:[S2]

$$CI(\%) = 100\left[\frac{(I_{002} - I_{am})}{I_{002}}\right]$$

where I_{002} is the intensity of the principal cellulose peak at 2θ = 22.7° and I_{am} is the intensity attributed to amorphous cellulose given at 2θ = 18°. The initial CNFs crystallinity was approximately 48.91% and it remained relatively constant after tip sonication (49.82%), proving that the proposed treatment does not affect cellulose crystal structure.

Table S2. CNFs and peptides concentrations used in the preparation of the hybrid samples, with the peptide molar concentration depending on the specific sequence.

CNFs concentration (wt%)	Peptide concentration (wt%)	Peptide molar concentration range (mM)
0.8	0.01	0.13 – 0.15
0.8	0.025	0.31 – 0.37
0.8	0.05	0.63 – 0.74
0.8	0.075	0.94 – 1.12
0.8	0.1	1.26 – 1.5

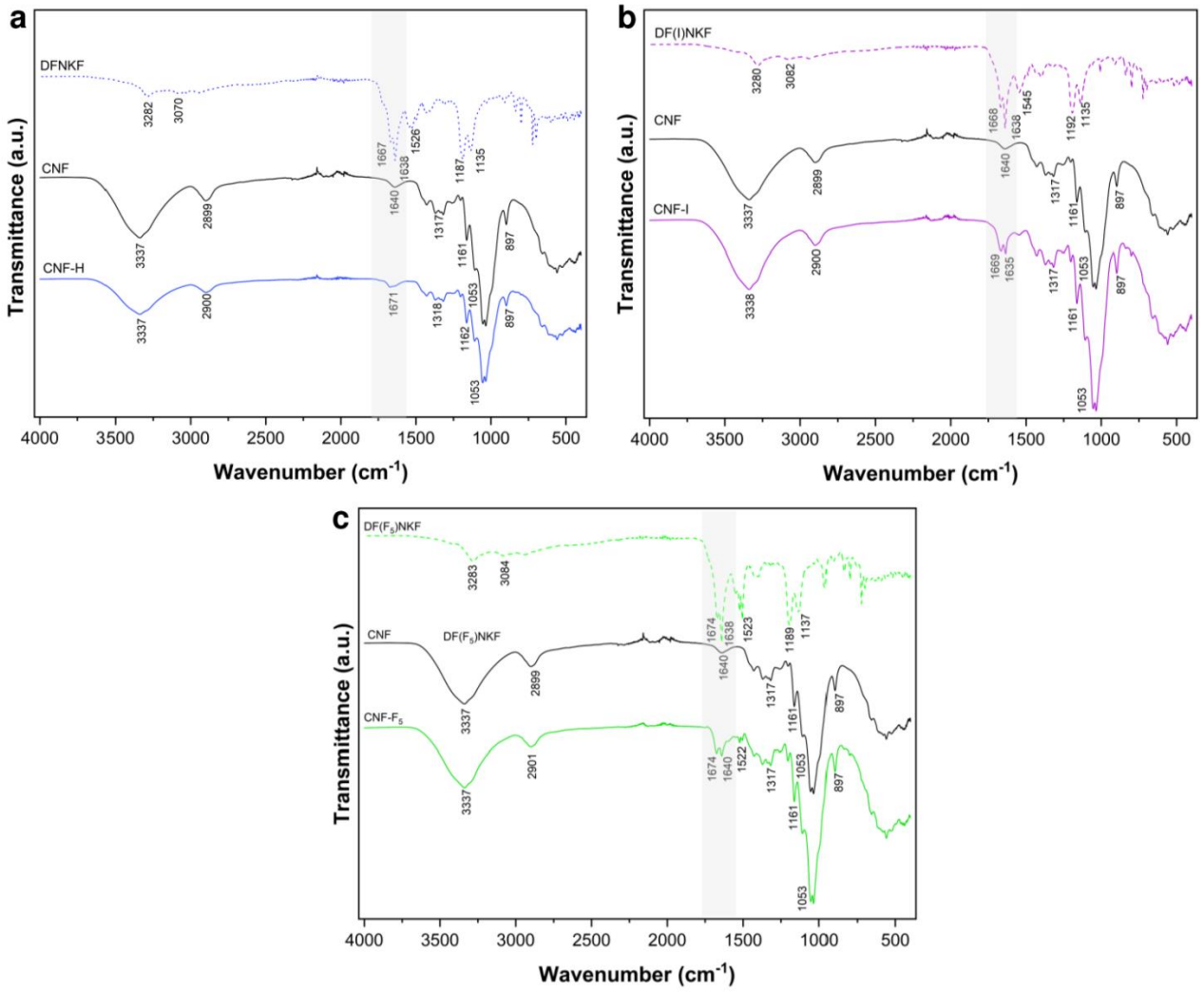

Figure S6. IR spectra of lyophilized hydrogels with 0.05 wt% a) DFNKF, b) DF(I)NKF and c) DF(F_5)NKF compared to neat nanocellulose. The samples displayed peaks characteristic for both nanocellulose and peptides, indicating the presence of both uniformly distributed in the system. The strong vibrational bands at 3337, 2900 and 1053 cm^{-1} are associated to the -OH, C-H, and C-O-C groups, typical of cellulosic substrates[S1]. At the same time, the correct integration of the peptides in the samples was confirmed by the appearance of strong vibrational bands at ~1600-1700 cm^{-1} and ~1540 cm^{-1} attributed to amide I and amide II modes, respectively.[S3]

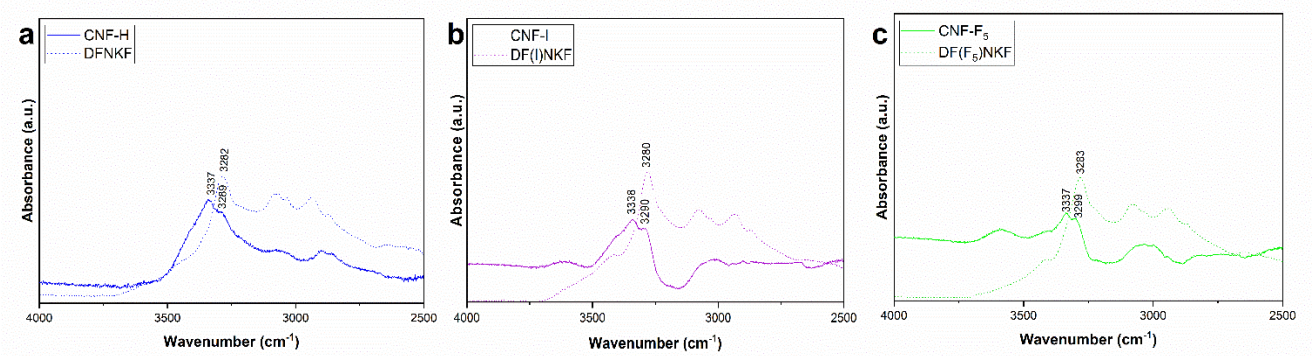

Figure S7. N-H stretching region in the FTIR spectra of a) CNF-H, b) CNF-I and c) CNF-F_5 at 0.05 wt% peptide content after substracting the contribute of neat CNF 0.8 wt%. Compared to the peptides alone, the N-H bands of DFNKF, DF(I)NKF and DF(F_5)NKF resulted to be blue-shifted of 7 cm^{-1}, 10 cm^{-1} and 16 cm^{-1}, respectively, after complexation with CNF.

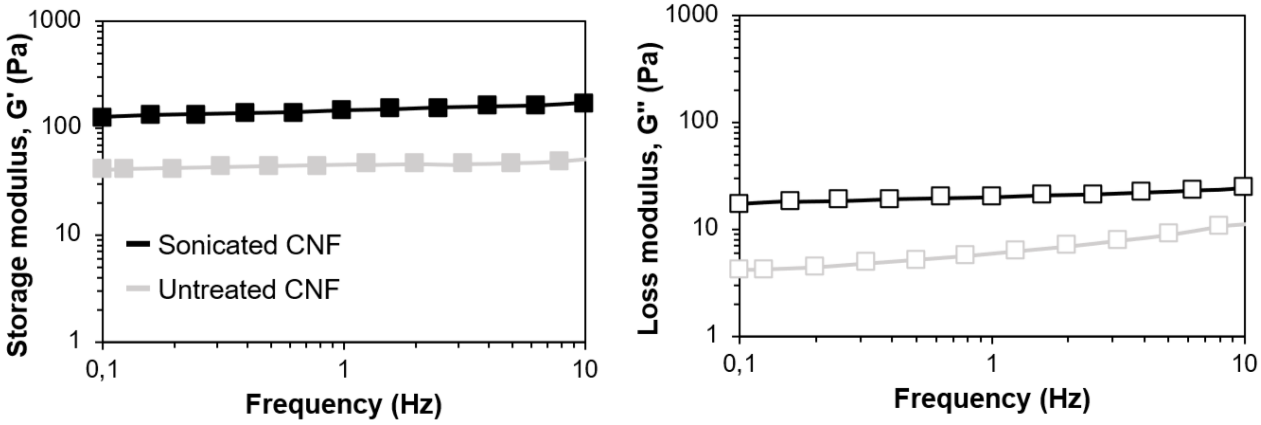

Figure S8. Effect of sonication on the rheological properties of 0.8% w/w CNF suspension.

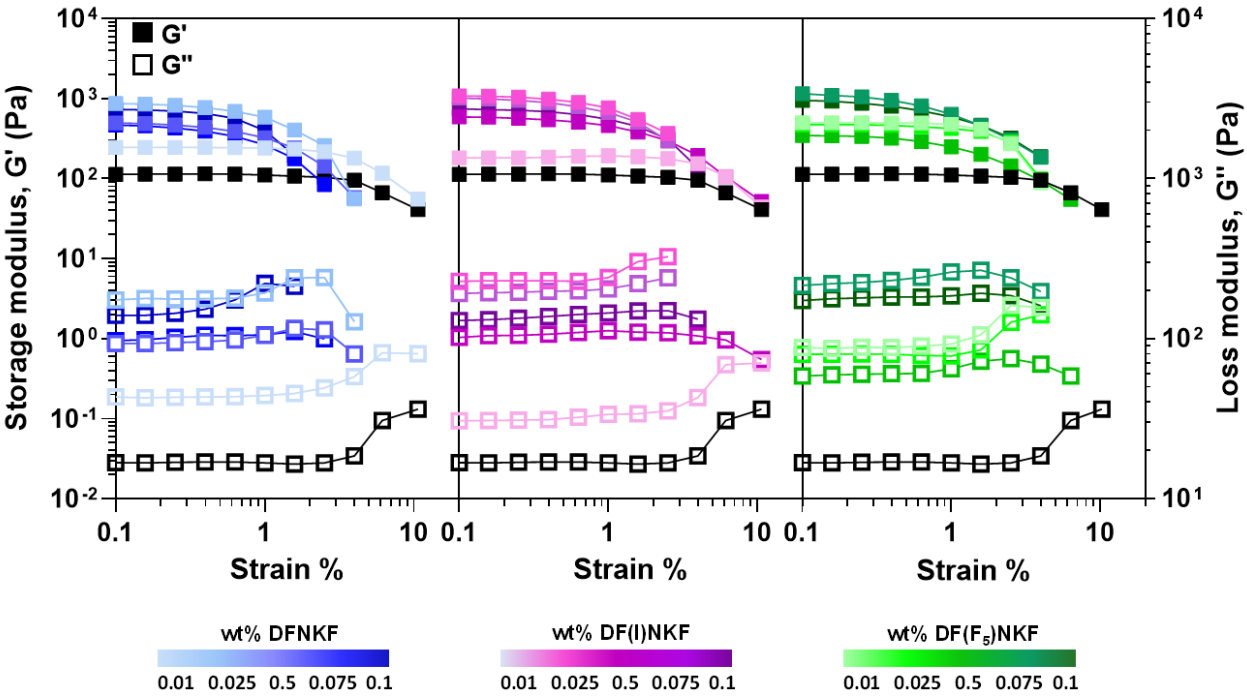

Figure S9. Amplitude sweep measurements of the composite hydrogels, comparing the DFNKF-based (in blue), DF(I)NKF-based (in violet) and DF(F_5)NKF-based (in green) systems with neat CNF (in black).

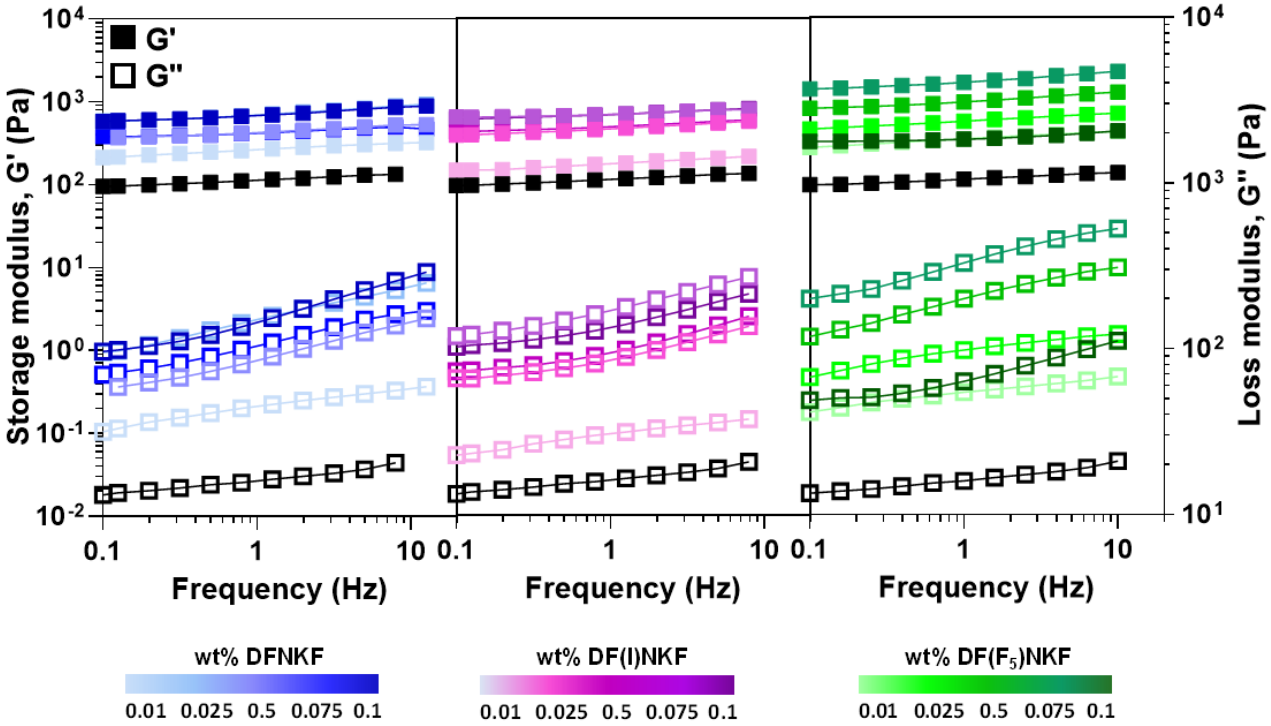

Figure S10. Frequency sweep measurements of the composite hydrogels, comparing the DFNKF-based (in blue), DF(I)NKF-based (in violet) and DF(F_5)NKF-based (in green) systems with neat CNF (in black).

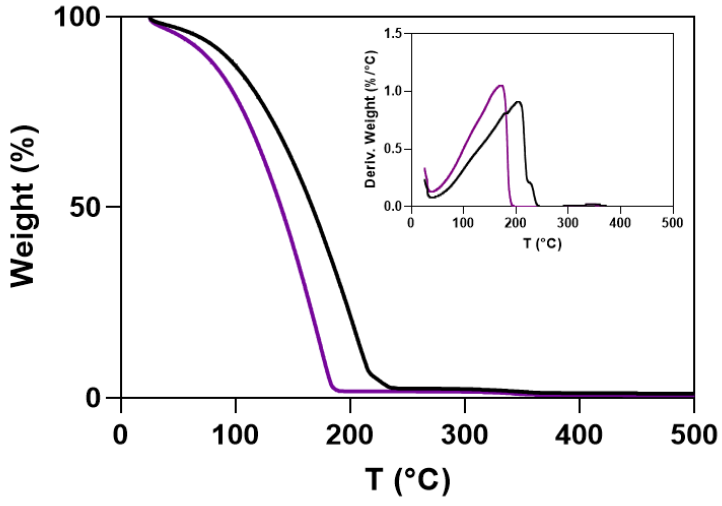

Figure S11. TGA measurement of 0.8 wt% CNF hydrogel with 0.05 wt% DF(I)NKF compared to neat CNF. The main weight loss is associated to water evaporation, with the maximum evaporation rate reached at lower temperatures in the composite with respect to CNF only. This result supports the importance of the impact of DF(I)NKF addition on CNF-water interaction, suggesting that, upon CNF-peptides complexation, the cellulose hydration layer is perturbated and water molecules are more easily released.[S4,S5]

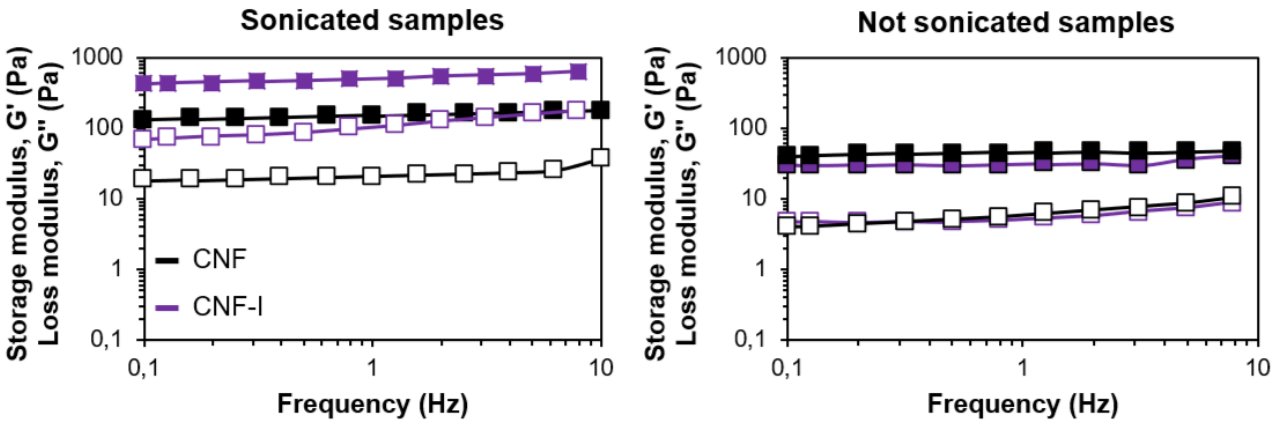

Figure S12. Effect of sonication on rheological properties of the composite with 0.05% w/w DF(I)NKF, highlighting the fundamental role of the ultrasound treatment for the increase of both dynamic moduli.

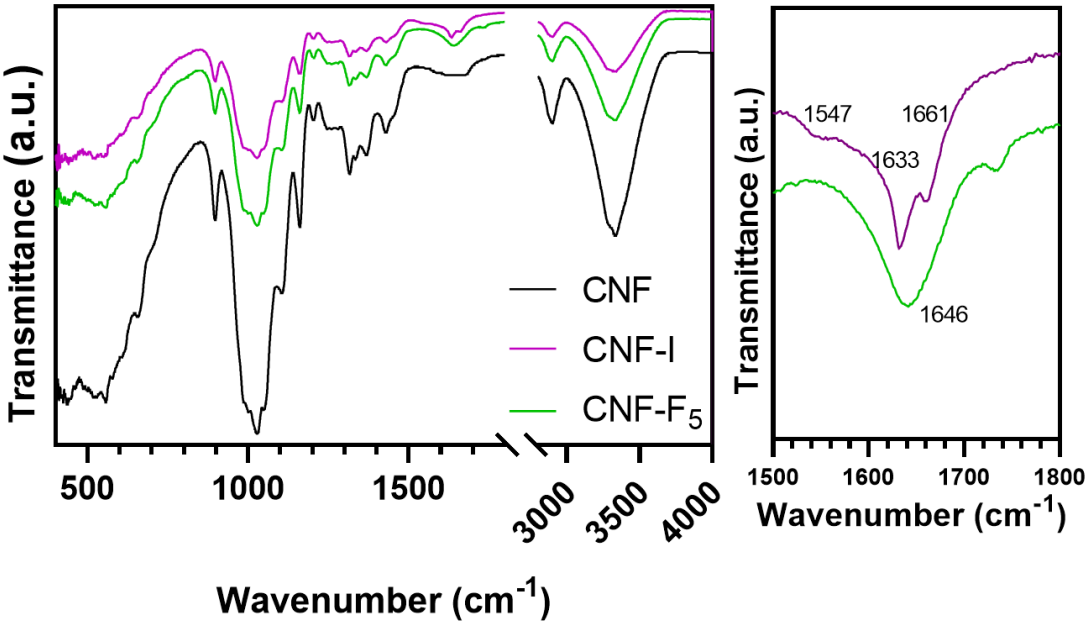

Figure S13. IR spectra of composite films with 0.1 wt% peptide content, highlighting the amide region where distinguishible DF(I)NKF and DF(F_5)NKF peaks are present.

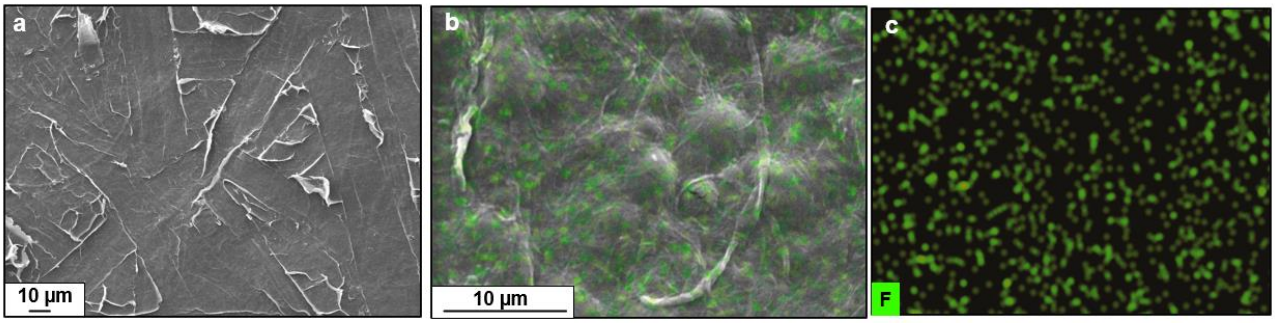

Figure S14. SEM images of a) neat CNF film and b) CNF-F_5 film at 0.1% w/w peptide concentration with overlapped fluorine distribution, with corresponding fluorine elemental map (c).

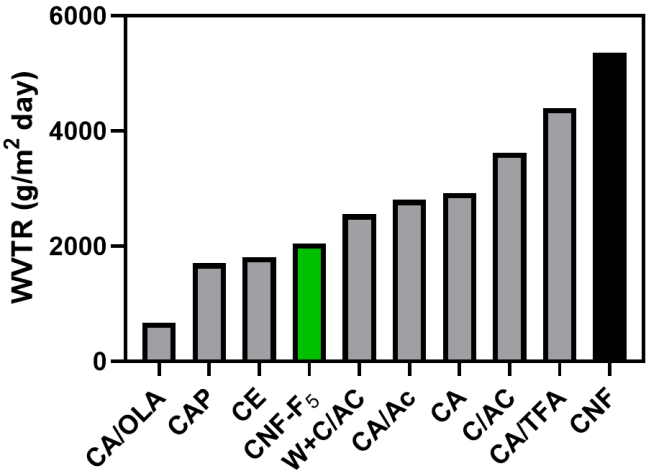

Figure S15. Water vapor transmission rates of common cellulose derivatives, highlighting the enhanced barrier properties obtained with the CNF-F_5 composite film, characterized by WVTR values comparable to industrially relevant cellulose materials. Labels: CA/OLA, Cellulose acetate-oleic acid; CAP, Cellulose acetate propionate; CE, Cellulose esters; W+C/AC, Wax+Cellulose-aleuritic acid; CA/Ac, Cellulose acetate/Acetone; CA, Cellulose acetate; C/AC, Cellulose-aleuritic acid; CA/TFA, cellulose acetate/TFA.[S6,S7]

References

S1 Foster, E. J.; Moon, R. J.; Agarwal, U. P.; Bortner, M. J.; Bras, J.; Camarero-Espinosa, S.; Chan, K. J.; Clift, M. J. D.; Cranston, E. D.; Eichhorn, S. J.; Fox, D. M.; Hamad, W. Y.; Heux, L.; Jean, B.; Korey, M.; Nieh, W.; Ong, K. J.; Reid, M. S.; Renneckar, S.; Roberts, R.; Shatkin, J. A.; Simonsen, J.; Stinson-Bagby, K.; Wanasekara, N.; Youngblood, J. Current Characterization Methods for Cellulose Nanomaterials. *Chemical Society Reviews* **2018**, 2609–2679. https://doi.org/10.1039/c6cs00895j.

S2 Segal, L.; Creely, J. J.; Martin, A. E.; Conrad, C. M. An Empirical Method for Estimating the Degree of Crystallinity of Native Cellulose Using the X-Ray Diffractometer. *Textile Research Journal* **1959**, *29* (10). https://doi.org/10.1177/004051755902901003.

S3 Kong, J.; Yu, S. Fourier Transform Infrared Spectroscopic Analysis of Protein Secondary Structures. *Acta Biochim Biophys Sin (Shanghai)* **2007**, *39* (8), 549-59. https://doi.org/10.1111/j.1745-7270.2007.00320.x.

S4 Arola, S.; Kou, Z.; Rooijakkers, B. J. M.; Velagapudi, R.; Sammalkorpi, M.; Linder, M. B. On the Mechanism for the Highly Sensitive Response of Cellulose Nanofiber Hydrogels to the Presence of Ionic Solutes. *Cellulose* **2022**, *29* (11), 6109–6121. https://doi.org/10.1007/s10570-022-04664-w.

S5 Kummer, N.; Giacomin, C. E.; Fischer, P.; Campioni, S.; Nyström, G. Amyloid Fibril-Nanocellulose Interactions and Self-Assembly. *J Colloid Interface Sci* **2023**, *641*, 338-347. https://doi.org/10.1016/j.jcis.2023.03.002.

S6 Shogren, R. Water Vapor Permeability of Biodegradable Polymers. *J Environ Polym Degrad* **1997**, *5* (2), 91-95. https://doi.org/10.1007/BF02763592.

S7 Kunam, P. K.; Ramakanth, D.; Akhila, K.; Gaikwad, K. K. Bio-Based Materials for Barrier Coatings on Paper Packaging. *Biomass Conversion and Biorefinery* **2022**. https://doi.org/10.1007/s13399-022-03241-2.